

Quantitative Proteomics Illuminates a Functional Interaction between mDia2 and the Proteasome

Tadamoto Isogai,^{†,||} Rob van der Kammen,^{†,||} Onno B. Bleijerveld,[§] Soenita S. Goerdal,[⊥] Elisabetta Argenzio,[‡] A. F. Maarten Altelaar,^{*,⊥,||,§} and Metello Innocenti^{*,†}

[†]Division of Molecular Genetics, [‡]Division of Cell Biology I, and [§]NKI Mass Spectrometry and Proteomics Facility, The Netherlands Cancer Institute, 1066 CX Amsterdam, The Netherlands

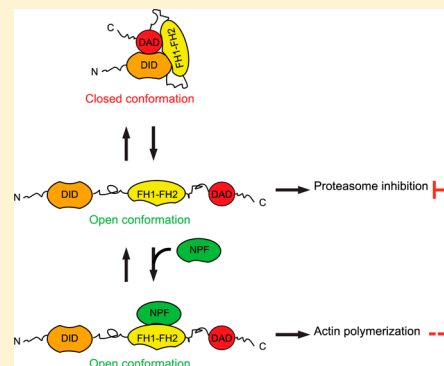
[⊥]Biomolecular Mass Spectrometry and Proteomics Group, Bijvoet Center for Biomolecular Research and Utrecht Institute for Pharmaceutical Sciences, Utrecht University, 3584 CH Utrecht, The Netherlands

^{||}Netherlands Proteomics Centre and Cancer Genomics Centre, 3584 CH Utrecht, The Netherlands

S Supporting Information

ABSTRACT: Formin mDia2 is a cytoskeleton-regulatory protein that switches reversibly between a closed, autoinhibited and an open, active conformation. Although the open conformation of mDia2 induces actin assembly thereby controlling many cellular processes, mDia2 possesses also actin-independent and conformation-insensitive scaffolding roles related to microtubules and p53, respectively. Thus, we hypothesize that mDia2 may have other unappreciated functions and regulatory modes. Here we identify and validate proteasome and Ubiquitin as mDia2-interacting partners using stable isotope labeling with amino acids in cell culture-based quantitative proteomics and biochemistry, respectively. Although mDia2 is ubiquitinated, binds ubiquitinated proteins and free Ubiquitin, it is not a proteasome substrate. Surprisingly, knockdown of mDia2 increases the activity of the proteasome in vitro, whereas mDia2 overexpression has opposite effects only when it adopts the open conformation and cannot induce actin assembly. Consistently, a combination of candidate and unbiased proteome-wide analyses indicates that mDia2 regulates the cellular levels of proteasome substrate β -catenin and a number of ubiquitinated actin-regulatory proteins. Hence, these findings add more complexity to the mDia2 activity cycle by showing that the open conformation may control actin dynamics also through actin-independent regulation of the proteasome.

KEYWORDS: quantitative proteomics, mass spectrometry, SILAC, affinity purification, biochemistry, Formin



INTRODUCTION

mDia2 (mouse homologue of Diaphanous 2) is a member of the Diaphanous-related Formin (Drf)-family of proteins whose hallmark is a Diaphanous autoregulatory domain (DAD) located in the C-terminus. This domain is positioned after the Formin homology (FH) FH1 and FH2 domains, which characterize all Formins.¹ The FH2 domain of mDia2 forms donut-shaped antiparallel dimers that nucleate linear actin filaments and also regulate elongation thereof by associating processively with the barbed ends.² In addition, the FH1–FH2 region of mDia2 has been recently shown to interact directly with and stabilize microtubules independently of its effects on actin.³

The N-terminus of mDia2 encompasses a basic domain (BD) followed by a GTPase-binding domain (GBD) to which activated Rho A-C and F bind.⁴ At variance with all other Drf proteins, mDia2 possesses also a partial CRIB (Cdc42/Rac interactive binding) domain that mediates direct binding to activated Cdc42.⁵ Downstream of it, a Diaphanous inhibitory domain (DID) and a dimerization domain (DD) may regulate both the tertiary and quaternary structure of mDia2.¹

The DID has been shown to bind to the DAD, and this interaction prevents the FH2 domain from promoting actin nucleation both in vitro and in vivo. Thus, the DID and DAD fulfill an important regulatory function that maintains Drfs in an autoinhibited or “closed” state.^{6,7} Mutation of crucial amino acids, such as the M1041-to-A substitution, disrupts the DID-binding abilities of DAD and forcefully keeps mDia2 in an “open”, active state bypassing regulatory signals.⁸ Among them are activated Rho proteins whose binding to the GBD induces a structural rearrangement in the adjacent DID that displaces the DAD and enables mDia2 to affect actin dynamics.

Regulation of actin dynamics by active mDia2 has been implicated in filopodium,^{9,10} bleb^{11,12} and invadopodium formation,¹³ cell invasion,^{13–15} erythropoiesis,¹⁶ vesicle trafficking,¹⁷ cytokinesis,¹⁸ and actin-dependent gene transcription.¹⁹

Regulation of microtubule dynamics by mDia2 may be either a direct or an indirect actin-independent effect of mDia2 because mDia2 can stabilize microtubules in vitro and also interacts with

Received: August 5, 2016

Published: October 21, 2016



a number of microtubule-regulatory proteins in cells.^{3,20} Remarkably, this seems to be a conformation-insensitive function of mDia2 as both active and autoinhibited mDia2 are able to promote formation of stable microtubules.^{3,21} Interestingly, an actin-independent and conformation-insensitive scaffolding role for mDia2 in p53 regulation, which links this Formin to the Ubiquitin proteasome system (UPS), has also been recently reported.²² Taken together, these findings suggest that the switch between the closed and the open conformation may not necessarily correspond to an on/off switch in the mDia2 activity cycle. In addition, both conformations of mDia2 may possess functionally inactive and active states. Analogously to the regulatory mechanism controlling actin polymerization by mDia2, interacting proteins and post-translational modifications likely govern the transition from the inactive to the active state associated with the unconventional functions of mDia2. As dysregulation of mDia2 is linked to human disease,^{23,24} it is of vital importance to elucidate in full the modes of action of mDia2.

Here we have exploited stable isotope labeling with amino acids in cell culture (SILAC)^{25,26} and affinity purification (AP) coupled to mass spectrometry (MS) to understand whether mDia2 has other unconventional functions and regulatory modes. By coupling this discovery tool with bioinformatics, we identify several new proteasome subunits and Ubiquitin as mDia2-interacting partners. In addition to validating these interactions biochemically, we show that mDia2 is a ubiquitinated protein and binds to both conjugated and free Ubiquitin. Yet, we find that mDia2 levels are not regulated by proteasome-mediated degradation. Rather, complementary loss-of-function and gain-of-function studies suggest that mDia2 inhibits the proteasome when it adopts the open conformation without regulating actin dynamics. Finally, the observation that β -catenin levels and those of a number of ubiquitinated actin-regulatory proteins are reduced in the mDia2 knockdown cells suggests that the interaction between mDia2 and the proteasome has a physiological relevance.

In summary, the tie between mDia2 and the proteasome sheds new light on the emerging actin-independent roles of mDia2 in the UPS. Most importantly, these findings suggest that the open conformation of mDia2 controls actin dynamics through both actin polymerization and actin-independent regulation of the proteasome.

■ EXPERIMENTAL PROCEDURES

Chemicals and Reagents

High-glucose DMEM supplemented with pyruvate and Gluta-Max, Lipofectamine, and Colloidal Blue Staining Kit were from Invitrogen. Stable isotope-labeled amino acids were from Silantes. SILAC DMEM with high glucose was from PAA Laboratories. FuGENE6 was from Roche. GelCode Blue Stain Reagent was obtained from Thermo Scientific. Microcon YM30 filter units were obtained from Millipore. QuikChange II Site-Directed Mutagenesis Kit was from Stratagene. Suc-L-L-V-Y-AMC was from Bachem, Lactacystin was from Cayman Chemicals, and Protease inhibitor EDTA-free cocktail was from Roche. If not otherwise specified, all other chemicals were from Sigma-Aldrich.

Expression Vectors

pCDNA3-Flag mDia2 (WT, IA, MA, and IAMA) were previously described.²² pGEX mDia2 was previously described.⁹ pCDNA3-Flag mDia2 3KR was generated by polymerase chain reaction using QuikChange II Site-directed Mutagenesis kit and sequence verified. Primer sequences with mutations

highlighted in capital were as follows: K130R: 5'-agacttcggtatca-Gaaagaatggtgatgcagctac-3'; K796R: 5'-aggtgaacaacatca-Gacctgacatcatggct-3' and K810R: 5'-ctgcgaggagatcaGgaagagcaaggcttt-3'. pCDNA3-HA-Ubiquitin was from E. Citterio. pCDNA3-LMP2-EGFP was a kind gift from J. Neefjes. pXJ41-mSUG1/Rpt6-Flag was from A. Bertolotti. pIRES-hrGFP1a vectors, expressing FLAG-tagged proteasome subunits PSMA5, PSMA6, and PSMA7, were from N. A. Barlev.

Cell Culture, Transfections, and Knockdowns

293T and HeLa cells were cultured in DMEM supplemented with 10% heat-inactivated FCS. 293T cells were transfected using a standard calcium phosphate protocol. HeLa cells were transfected with FuGENE6 or Lipofectamine according to the manufacturer's instructions. Transient mDia2 knockdown cells were generated as previously described^{9,27} and assessed 48 h post-transfection. Stable mDia2 knockdown HeLa cells were obtained by lentiviral infection using the MISSION TRC shRNA TRCN0000150903 and subsequent selection with puromycin (Invitrogen). Stable mDia1 knockdown HeLa cells were previously described.²⁸

SILAC and mDia2 Immunoprecipitation from Labeled Cells

293T cells were gradually adapted to growth in SILAC medium by culturing them in a mixture of SILAC (either light or heavy) and normal medium. Starting from a 1:3 v/v ratio, the amount of SILAC medium was increased every other day first to 1:1, then to 3:1, and finally to full SILAC medium. 293T cells were grown in biological duplicate for at least six cell doublings in SILAC medium to achieve a complete labeling and afterward transfected with Flag-tagged mDia2 (either the wild type or the MA mutant) or empty vector. Transfections were performed so that heavy (H)/light (L) label swaps were introduced. Cell lysates were prepared using JS buffer as previously described.^{9,27,29} One and one-half milligrams of cell lysates (approximately 200 μ L) was immunoprecipitated using a bed volume of about 35 μ L of anti-Flag M2 Affinity gel (Sigma-Aldrich) for 2 h at 4 °C. Beads were washed three times in NET buffer (50 mM Tris-HCl pH 7.6, 150 mM NaCl, 5 mM EDTA, and 0.1% Triton X-100) supplemented with protease inhibitor cocktail (Roche), 5 mM NaF, and 1 mM NaVO₄. Proteins were eluted with Laemmli buffer, and SILAC H/L-labeled eluates were mixed and separated by SDS-PAGE (NuPage 4–12% Bis-Tris gradient gel (Invitrogen)). The gel was fixed and stained with Colloidal Blue according to the manufacturer's instructions.

Affinity Purification of Ubiquitinated Proteins, Whole-Proteome, and Ubiproteome Analyses

For label-free quantitation of whole proteomes and ubiproteomes, control and mDia2 knockdown HeLa cells were seeded in 10 cm Petri dishes and, the day after, lysed using RIPA buffer (50 mM Tris-HCl pH 7.6, 150 mM NaCl, 2 mM EDTA, 1% NP-40, 0.5% C₂₄H₃₉NaO₄ (sodium deoxycholate), 0.1% SDS) supplemented with EDTA-free protease inhibitors (Roche), phosphatase inhibitors, and 5 mM N-Ethylmaleimide (NEM). Lysates were spun for 10 min at 15 000 rpm at 4 °C in a tabletop centrifuge to remove insoluble material, flash-frozen in liquid nitrogen, and slowly thawed on ice.

For proteome-wide quantitation, aliquots comprising 100 μ g of total proteins were digested using the FASP procedure (protocol 2) described by Wisniewski et al.,³⁰ with Microcon YM30 filter units, and Lys-C (Wako) (4 h at 37 °C, 1:100 enzyme/protein ratio) and Trypsin (Promega) (o/n at 37 °C, 1:50 enzyme/protein ratio) as proteolytic enzymes. Peptides eluted

from the FASP filter units were desalted on a Sep-Pak C18 cartridge (Waters), dried down in a speed vacuum centrifuge, and stored at -80°C until subjected to LC-MS/MS analysis.

For affinity purification of ubiquitinated proteins, lysates (1 mg) were precleared with Protein-G Sepharose 4 Fast Flow (GE Healthcare) for 30 min at 4°C under gentle agitation, and then each supernatant was incubated with $6\text{ }\mu\text{g}$ of anti-FK2 antibodies and Protein-G Sepharose beads for 2 h at 4°C under gentle agitation. Immunocomplexes were washed four times with RIPA buffer supplemented with protease and phosphatase inhibitors and 5 mM N-ethylmaleimide (NEM) and once with storage buffer (50 mM Tris-HCl pH 7.6, 150 mM NaCl). Beads were dried, flash-frozen, and stored at -80°C . For elution, beads were reconstituted in XT sample buffer (Bio-Rad) and heated at 95°C for 7 min. Eluates were subsequently cleared and concentrated into a small protein band by short, partial SDS-PAGE separation. The gel was stained with GelCode Blue stain reagent, followed by excision of the gel bands, reduction of the proteins with 6.5 mM DTT (56°C , 1 h), and alkylation with 54 mM 2-chloroacetamide (30 min, RT). Proteins were digested with sequencing grade trypsin (3 ng/ μL) overnight at 37°C . Peptides were extracted with acetonitrile, dried down in a speed vacuum centrifuge, and reconstituted in 10% formic acid prior to mass spectrometry analysis.

Mass Spectrometry

Reduction and alkylation of SILAC-labeled proteins were performed in gel with 6.5 mM DTT (56°C , 1 h) and 54 mM 2-chloro-iodoacetamide (dark, RT, 30 min), respectively, after which digestion was performed with sequencing-grade trypsin (3 ng/ μL) (Promega) overnight at 37°C . Peptides were extracted with 100% ACN. The samples were analyzed on an LTQ Orbitrap (Thermo Scientific, Bremen) connected to an Agilent 1200 HPLC system. The nanoLC was equipped with a 20 mm 100 μm i.d. Reprosil C18 trap column and a 400 mm 50 μm i.d. Reprosil C18 analytical column (Dr Maisch, Ammerbuch-Entringen, Germany) all packed in-house. Solvent A consisted of 0.1 M acetic acid (Merck) in deionized water (Milli-Q, Millipore), and solvent B consisted of 0.1 M acetic acid in 80% acetonitrile (Biosolve). Trapping was performed at a flow of 5 $\mu\text{L}/\text{min}$ for 10 min, and the fractions were eluted using a flow rate passively split to 100 nL/min. SILAC-labeled peptides were separated in a 60 min gradient consisting of 10 min solvent A; 10–40% solvent B within 30 min; 100% solvent B for 2 min; and final equilibration with 15 min solvent A. The mass spectrometer was operated in positive ion mode and in data-dependent mode to automatically switch between MS and MS/MS. The three most intense ions in the survey scan (350–1500 m/z , resolution 60 000, AGC target $5e5$) were fragmented by collision-induced dissociation (CID) in the linear ion trap (AGC target $1e4$), with the normalized collision energy set to 35%. The signal threshold for triggering an MS/MS event was set to 500 counts. Charge state screening was enabled, and precursors with unknown charge state or a charge state of 1 were excluded. Dynamic exclusion was enabled (exclusion size list 500, exclusion duration 25 s).

For identification of ubiquitination sites on affinity-purified Flag-tagged mDia2, in-gel digests were analyzed by LC-MS/MS on an LTQ-Orbitrap Velos instrument (Thermo Scientific) using a decision-tree method with the orthogonal fragmentation methods, HCD and ETD.³¹ Chromatography (100 min gradient) and mass spectrometry were performed as described previously.^{31,32} All biological replicates were analyzed with two technical LC-MS/MS replicates.

For label-free analysis of whole-proteome and anti-FK2-eluate digests, peptides were separated using a Proxeon nLC 1000 system (Thermo Scientific, Bremen) fitted with an analytical column (ReproSil-Pur 120 C18-AQ 2.4 μm (Dr. Maisch GmbH); 75 μm \times 500 mm), packed in-house. The outlet of the analytical column was coupled directly to a Thermo Orbitrap Fusion hybrid mass spectrometer (Q-OT-qIT, Thermo Scientific) using the Proxeon nanospray source. Nanospray was achieved using a distally coated fused silica tip emitter (generated in-house, o.d. 375 μm , i.d. 20 μm) operated at 2.1 kV. Solvent A was 0.1% formic acid/water, and solvent B was 0.1% formic acid/ACN. One microgram aliquots of whole proteome digests were eluted from the analytical column at a constant flow of 250 nL/min in a 270 min gradient, which contained a 5 min start section from 2 to 3% solvent B, a linear increase to 24% solvent B in 185 min, a 40 min increase to 35% solvent B, a 20 min increase to 60% solvent B, a 5 min increase to a 5 min plateau of 95% solvent B, and finally a 5 min decrease to 5 min equilibration at 5% solvent B. Aliquots (25%) of anti-FK2-eluate digests were separated in a 90 min gradient comprising a 71 min linear gradient from 6 to 30% solvent B, followed by a 18 min plug of 100% solvent B. Survey scans of peptide precursors from m/z 375–1500 were performed at 120 K resolution with a 4×10^5 ion count target. MS/MS was performed by quadrupole isolation at 1.6 Th, followed by HCD fragmentation with normalized collision energy of 33 and ion trap MS² fragment detection. The MS² ion count target was set to 10^4 , and the maximal injection time was set to 50 ms. Only precursors with charge state 2–6 were sampled for MS². Monoisotopic precursor selection was turned on; the dynamic exclusion duration was set to 30 s with a 10 ppm tolerance around the selected precursor and its isotopes. The instrument was run in top speed mode with 3 s cycles. All biological replicates were analyzed with two technical LC-MS/MS replicates.

MS Data Analysis

Raw data were analyzed by MaxQuant (version 1.5.0.30)³³ using standard settings. MS/MS data were searched against the human Swissprot database (20 192 entries, release 2015_02) complemented with a list of common contaminants and concatenated with the reversed version of all sequences. The minimum peptide length was set to seven amino acids. The initial maximum allowed mass tolerance was 20 ppm for peptide masses, followed by 4.5 ppm in the main search and 0.5 Da for fragment ion masses. False discovery rates for peptide and protein identification were set to 1%. Ion scores >40 were required for identification of modified peptides. Trypsin/P was chosen as cleavage specificity allowing two missed cleavages. Carbamidomethylation (C) was set as a fixed modification, while oxidation (M) was used as variable modification. No labels (Arg0/Lys0) and Arg10/Lys8 were selected for light and heavy quantification label, respectively. The generated “proteingroups.txt” table was filtered for contaminants, reverse hits, and a minimum of two unique peptides to be used for protein quantitation. H/L ratios were \log_2 -transformed in Perseus, and label swaps were plotted against each other for both the WT/Ctrl and MA/Ctrl mDia2 IPs. On the basis of the distributions of the H/L ratios, $\log_2 [\text{H/L}] \geq 1$ and $\log_2 [\text{H/L}] \leq -1$ were taken as cutoff to discriminate between true and false interactions.

For LFQ whole-proteome data, LFQ intensities (3 biological replicate values for both control KD and mDia2 KD cells) were \log_2 -transformed in Perseus, after which proteins were filtered for at least four valid values (out of 6 total control KD/mDia2 KD replicates). Proteins with three valid values in only one of the

sample groups were considered as a separate “on/off” group. Missing values were replaced by imputation based on a normal distribution using a width of 0.3 and a downshift of 1.8.³⁴ Differentially expressed proteins were determined using a permutation-based FDR-corrected *t*-test (threshold: $P = 0.05$ and $S_0 = 0.23$). The control KD and mDia2 KD ubiquitomes were determined using biological duplicates. LFQ analysis was performed as described above, with the difference that robust “on/off” proteins were defined by means of two valid LFQ intensity values in only one of the two sample groups. Differential abundance of ubiquitinated proteins in the anti-FK2 IPs was assessed by manual inspection of protein dots deviating from the bulk cloud in the correlation plots of the biological replicates.

Ubiquitination sites on affinity purified Flag-tagged mDia2 were identified by generating peak lists from the raw data files using the Proteome Discoverer software package version 1.4.1.14 (Thermo Scientific). Peptide identification was performed by searching the peak list against a concatenated target-decoy Swissprot database containing *Mus musculus* protein sequences (release 2015_04, 16 714 target sequences) using the Mascot search engine version 2.5 (Matrix Science, London, U. K.) via the Proteome Discoverer interface. The search parameters included the use of trypsin as proteolytic enzyme allowing up to a maximum of two missed cleavages. Carbamidomethylation of Cysteine was set as a fixed modification, whereas oxidation of methionine and the GG(K) ubiquitination tag on lysine residues were set as variable modifications. Precursor mass tolerance was initially set at 50 ppm, while fragment mass tolerance was set at 0.05 Da for HCD and ETD fragmentation in the Orbitrap. Subsequently, peptide identifications were filtered for Mascot score >20 until an FDR < 1% at peptide level was achieved.

The mass spectrometry data have been deposited to the ProteomeXchange Consortium³⁵ through the PRIDE partner repository (Project accession, PXD002066; Username, reviewer54687@ebi.ac.uk; Password, mrtfepq3).

Bioinformatic Analyses

Bioinformatic analyses were carried out using Ingenuity Pathways Analysis (IPA) (Qiagen). The mDia2-binding proteins, as well as the ubiquitome and the total proteome of the control and the mDia2 knockdown HeLa cells, were submitted for Biological function and Canonical Pathway Analysis to identify the pathways that were most significantly associated with the query among those present in the IPA library. The significance of the association between the data set and the canonical pathway was measured with two parameters: (1) the number of associated proteins from the data set that are assigned to a given canonical pathway, and (2) the Fischer's exact test determining the probability (*p*-value) that the association between the genes in the data set and the canonical pathway occurs by chance.

Gene Ontology (GO) analyses were done using the Database for Annotation, Visualization, and Integrated Discovery (DAVID) v6.7 to cluster redundant annotation terms.³⁶ Default annotation categories defined by DAVID were used, and Function Annotations were clustered with highest stringency as indicated. Full cluster reports are documented in Supplemental Table S-2 for the mDia2-binding proteins (with enrichment score >2 and Benjamini Hochberg *p*-value <0.05).

Protein Interaction Maps

Protein–protein interaction maps were built using the STRING protein–protein interaction database³⁷ and Cytoscape.³⁸ The STRING software assembles functional protein networks based

on compiled evidence. Obtained interaction maps were visualized in Cytoscape.

Standard Biochemical Assays

Expression and purification of GST and GST-mDia2 were done as previously described.^{9,29} Pull-down assays were performed as previously described:^{9,22,29} cleared cell lysates (500 μ g) expressing the protein of interest were incubated for 2 h at 4 °C with immobilized GST-fusion proteins (62.5 pmol). Beads were extensively washed and bound proteins eluted with Laemmli buffer. In all pull-down experiments, correct loading was always verified using Ponceau S (not shown). Co-immunoprecipitation experiments were performed as previously described,^{22,29} unless stated otherwise. For verification of mDia2 ubiquitination, total cell lysates were made in RIPA buffer supplemented with protease and phosphatase inhibitors and 5 mM NEM and underwent a freeze–thaw cycle. Immunoprecipitated complexes were washed four times with RIPA buffer. Total cell lysates were obtained as previously described,^{22,29} and 30 μ g was employed in all straight immunoblotting experiments. Purified recombinant Ubiquitin was a kind gift from T. Sixma.

Antibodies

Antibodies: mouse monoclonal anti-Flag M2 Affinity gel, anti-Flag M2, anti- β -actin (AC-15) (Sigma-Aldrich), mouse monoclonal anti-mDia1 and anti- β -catenin (BD Transduction Laboratories), rabbit monoclonal anti-PSMA1 (Epitomics), rabbit polyclonal anti-Rpt1 (Abcam), mouse monoclonal antimyc 9E10, anti-HA-11 and anti-Ub (P4D1) (Covance), mouse monoclonal anti-NEK2A (BD Biosciences), mouse monoclonal anti-FK2 (Enzo), rabbit polyclonal anti-mDia2 and anti-EGFP sera were previously described.^{22,27}

Proteasome Activity Assay

The activity of the proteasome was measured exploiting a fluorogenic substrate (Suc-L-L-V-Y-AMC) and an established protocol.³⁹ Either 6 or 3 μ g of cleared cells lysates was used to determine the chymotrypsin-like activity of the proteasome upon knockdown and overexpression of mDia2. AMC fluorescence was measured at 20 °C in a SAFAS flx XENIUS spectrofluorometer (excitation, 380 ± 5 nm; emission, 460 ± 10 nm; sampling rate, 13 s). In all instances, cells were pretreated for 4 h at 37 °C with either Lactacystin (10 μ M) or an equivalent volume of DMSO, as a control. Notably, Lactacystin abolished the cleavage of Suc-L-L-V-Y-AMC, which thereby showed the specificity of the assay. On the contrary, Lactacystin did not affect the cleavage of Ac-nLPnLD-amc and Boc-LSTR-amc thereby showing that the caspase-like and trypsin-like activities of the proteasome were below the detection limit. The proteasome activity was calculated as the initial rate of substrate cleavage, which corresponds to the slope of the lines obtained from spectrofluorometric measurements. This value was divided by two whenever obtained from the measurement of 6 μ g of lysate. Data in the bar graphs are represented as mean \pm SD from at least three independent experiments.

Statistical Analyses

Student's unpaired *t* test was employed. $P < 0.05$ was considered statistically significant. *P*-values reported by IPA and DAVID analyses were calculated by Fisher-Exact tests or FDR (Benjamini-Hochberg) method, respectively.

■ RESULTS

SILAC-Based Quantitative Proteomics Identifies the Proteasome and Ubiquitin as mDia2-Binding Partners

Wild-type mDia2 attains a punctate cytosolic and a faint nuclear pattern and does not alter the morphology of the actin cytoskeleton, whereas its active M1041-to-A mutant (hereafter referred to as mDia2 MA) promotes formation of filopodia and readily accumulates at the tip thereof.²² We transiently expressed Flag-tagged wild-type mDia2 and mDia2 MA in either heavy (H)- or light (L)-labeled 293T cells (Supplemental Figure S1A) and observed that both wild-type mDia2 and its MA mutant localized as indicated above (not shown). Given that the SILAC medium had no noticeable effects on mDia2 activity and the cytoskeleton, we performed forward and reverse SILAC label-swap experiments on cells expressing wild-type mDia2 (or the MA mutant) and the corresponding empty vector and used AP-MS to compile the interactomes of mDia2 (Supplemental Figure S1A).

Identified proteins (Supplemental Table S-1) were regarded as candidate mDia2-binding proteins only if their log₂ heavy-to-light (H/L) ratios in the label-swap scatter plots were ≥ 1 and ≤ -1 in the forward and reverse experiments, respectively (Supplemental Figure S1B,C). In this way, we identified 33 and 31 candidate interactors for the wild type and the MA mutant, respectively, and globally 47 nonredundant mDia2-binding proteins (Figure 1A and Supplemental Table S-1). Among them, 13 previously reported mDia2-binding proteins, including Profilin 1 and 2, VTA-1, CHMP5, and FBXO3,²² directly supported the validity of our results. In addition, the considerable overlap between the interactomes (36.2%) of wild-type and constitutively active mDia2 is consistent with our published findings²² and suggests that a large fraction of the identified interactions is independent of mDia2's conformation.

Protein ubiquitination pathway was both significantly enriched and highly represented in both interactomes (Figure 1B). This was further supported by GO analysis showing the enrichment of many Ubiquitin-related annotations (Figure 1C and Supplemental Table S-2). Although we identified a few proteasome subunits as potential mDia2-binding proteins in a previous study,²² only this approach evidenced a highly connected region comprising Ubiquitin and several proteasome subunits in the protein interaction map of both wild-type and active mDia2 (Figure 1D and E, respectively). The sum of these results suggests that mDia2 may bind to Ubiquitin and the proteasome and further corroborates the existence of a link between mDia2 and the UPS.²²

Validation of the Interaction between mDia2 and the Proteasome

Prompted by the these findings, we set out to validate the proteasome as a genuine mDia2-binding partner. In brief, we assessed the coprecipitation of endogenous 20S proteasome subunit PSMA1 and 19S proteasome subunit Rpt1 (also referred to as PSMC2) with Flag-tagged mDia2 and found that they bound to both wild-type mDia2 and the MA mutant (Figure 2A).

To corroborate these observations, we performed reciprocal coimmunoprecipitation experiments showing a specific interaction between mDia2 and both the 20S proteasome subunit PSMA7 (Figure 2B,C) or the 19S proteasome subunit Rpt6 (also referred to as PSMC5) (Figure 2D,E). As only the latter subunit was identified as a candidate mDia2-binding protein in our screen (Supplemental Table S-1), these results suggest that mDia2 can associate with the proteasome rather than with its

isolated subunits. Consistent with this notion, mDia2 interacted also with PSMA5 and PSMA6 (Figure 2C). The sum of these data strongly suggests that the proteasome is an mDia2-binding partner. Importantly, this interaction is not mediated by actin, which did not coprecipitate with either mDia2 or the proteasome under these conditions (Figure 2).

mDia2 Is Ubiquitinated and Binds Ubiquitinated Proteins

Given that the proteasome and Ubiquitin are genuine mDia2-binding proteins, we wondered whether mDia2 undergoes ubiquitination and binds to Ubiquitin or ubiquitinated proteins.

To test these hypotheses, we cotransfected HA-tagged Ubiquitin with either Flag-tagged mDia2 or a control empty vector and subsequently immunoprecipitated mDia2. Immunoblotting with anti-Flag antibodies revealed a main and a minor upward-shifted mDia2 band, the latter having a size compatible with monoubiquitinated mDia2 (Figure 3A). Anti-HA antibodies detected protein species covalently bound to HA-Ubiquitin that were very abundant in this region and formed a smear above it (Figure 3A). Moreover, there were distinct bands beneath mDia2, which may correspond to ubiquitinated mDia2 truncated/degraded products or ubiquitinated mDia2-binding proteins (Figure 3A). Taken together, these results suggest that mDia2 is polyubiquitinated or monoubiquitinated at multiple sites and may bind to ubiquitinated proteins. To strengthen this point, we omitted HA-Ubiquitin and repeated the experiment outlined above under conditions that either disrupt most noncovalent protein–protein interactions or only prevent the weak ones. Under the former conditions, we observed a smear recognized by the anti-Ubiquitin antibodies only in the region above wild-type and constitutively active mDia2 (Figure 3B). Conversely, the latter conditions resulted in the mDia2-based immunocomplexes having a pattern very similar to that observed upon coexpression of HA-Ubiquitin (Supplemental Figure S2).

Consistent with the notion that mDia2 is ubiquitinated, we identified three lysine residues displaying the K-GG signature⁴⁰ in the primary sequence of mDia2 (Supplemental Figure S3A,B). The finding that recombinant full-length GST-mDia2 pulled down high-molecular weight HA-Ubiquitin conjugates from cell lysates suggests that ubiquitination is not essential for mDia2 to associate with ubiquitinated proteins (Figure 3C).

mDia2 Associates Directly with Free Ubiquitin

mDia2's ability to interact with different ubiquitinated protein species may be partly due to mDia2 binding Ubiquitin in a non-covalent manner. To understand the nature of the interaction between mDia2 and Ubiquitin, we took advantage of purified recombinant full-length mDia2 and Ubiquitin and discovered that immobilized full-length GST-mDia2 pulled down soluble free Ubiquitin, whereas immobilized GST failed to do so (Figure 3D). This result suggests that mDia2 may function as a Ubiquitin receptor. Hence, ubiquitination of mDia2-binding proteins may create low-affinity binding sites that facilitate the interaction with mDia2.

mDia2 Regulates the Activity of the Proteasome

The proteasome contributes to proteostasis by mediating proteolytic degradation of many cytosolic proteins.⁴¹ Given that this process often involves the targeting of polyubiquitinated substrate proteins to the proteasome, interaction of ubiquitinated mDia2 with the proteasome may be a prelude to its disposal.

We tested this hypothesis using the irreversible proteasome inhibitor Lactacystin, which induced accumulation of genuine proteasome targets such as β -catenin and NEK2A⁴² (Figure 4A).

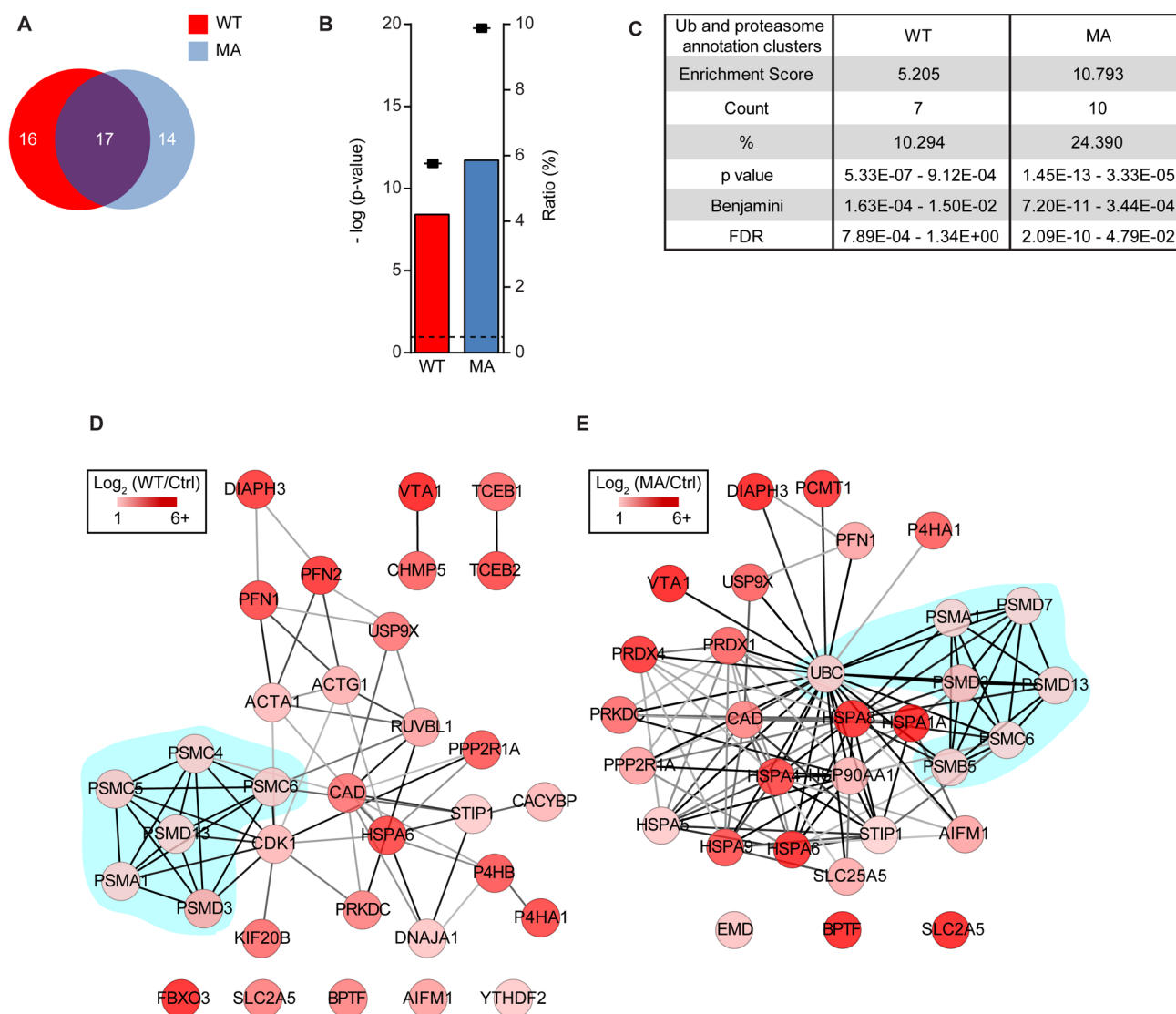


Figure 1. Proteasome takes center stage in the interactome of mDia2. (A) Overlap between the interactome of wild-type and active mDia2 is 36.2%. Venn diagram showing the number proteins unique to either wild-type (WT; red) or active (MA; blue) mDia2 as well as the number of the common ones (purple). Percentage of overlap was obtained as follows: common proteins (17)/total nonredundant proteins (47) \times 100 = 36.2%. (B) The link between mDia2 and the UPS is independent of mDia2 conformation. Bar graphs show ratios (% of the clustered proteins with respect to the total number of proteins belonging to the IPA protein ubiquitination pathway) and Fischer's Exact *t* test *p*-values (as log (*p*-value) indicated with a dot plot). Dashed black line marks the enrichment threshold. Of note, the IPA protein ubiquitination pathway is a top canonical pathway in the interactome of both wild-type (WT) and active (MA) mDia2 (not shown). (C) Ubiquitin and proteasome related GO terms are enriched in the interactome of both WT and MA mDia2. Functional annotations were clustered using DAVID as described in the [Experimental Procedures](#). (D) Interaction map of WT mDia2. Interaction map was built using only the binding proteins having a log₂ H/L ratio equal to or higher than 2 in both forward and reverse experiments ([Supplemental Table S-1](#)). Protein–protein interactions were extracted and visualized as indicated in the [Experimental Procedures](#), and unconnected proteins were added manually. Edge color represents the combined STRING score (0–1) computed by combining the probabilities from the different evidence channels after correction for the probability of random occurrence of the same interaction. Node color represents the log₂ ratio over control and is color-coded as depicted in the box. Light blue balloon encloses the highly connected region comprising several proteasome subunits. (E) Interaction map of constitutively active (MA) mDia2. Interaction map was built and represented as in panel D. Light blue balloon encloses the highly connected region comprising Ubiquitin and several proteasome subunits.

Although mDia2 can undergo proteasome-dependent degradation at the end of mitosis,⁴³ Lactacystin failed to affect mDia2 (or its paralog mDia1) in growing HeLa and 293T cells ([Figure 4A](#) and [ref 22](#), respectively). Similar results were obtained also with MG-132, a reversible inhibitor of the proteasome (data not shown). Thus, it seems unlikely that ubiquitination commits mDia2 for degradation outside mitosis.

We then raised the alternative hypothesis that mDia2 may regulate the function of the proteasome. Hence, we employed a fluorogenic substrate to measure proteolytic activity of the

proteasome³⁹ in control and mDia2 knockdown HeLa cells ([Figure 4B,C](#) and [Supplemental Figure S4A](#)). As expected, substrate cleavage augmented linearly over time and was completely abrogated by Lactacystin ([Figure 4D](#)). Surprisingly, the initial rate of substrate cleavage significantly increased upon either transient or stable knockdown of mDia2 ([Figure 4D,E](#) and [Supplemental Figure S4B,C](#), respectively). Interestingly, we noticed a reproducible decrease in β -catenin levels in the mDia2 knockdown cells, which was rescued by Lactacystin ([Figure 4F,G](#)). Of note, the knockdown of mDia1 did not affect

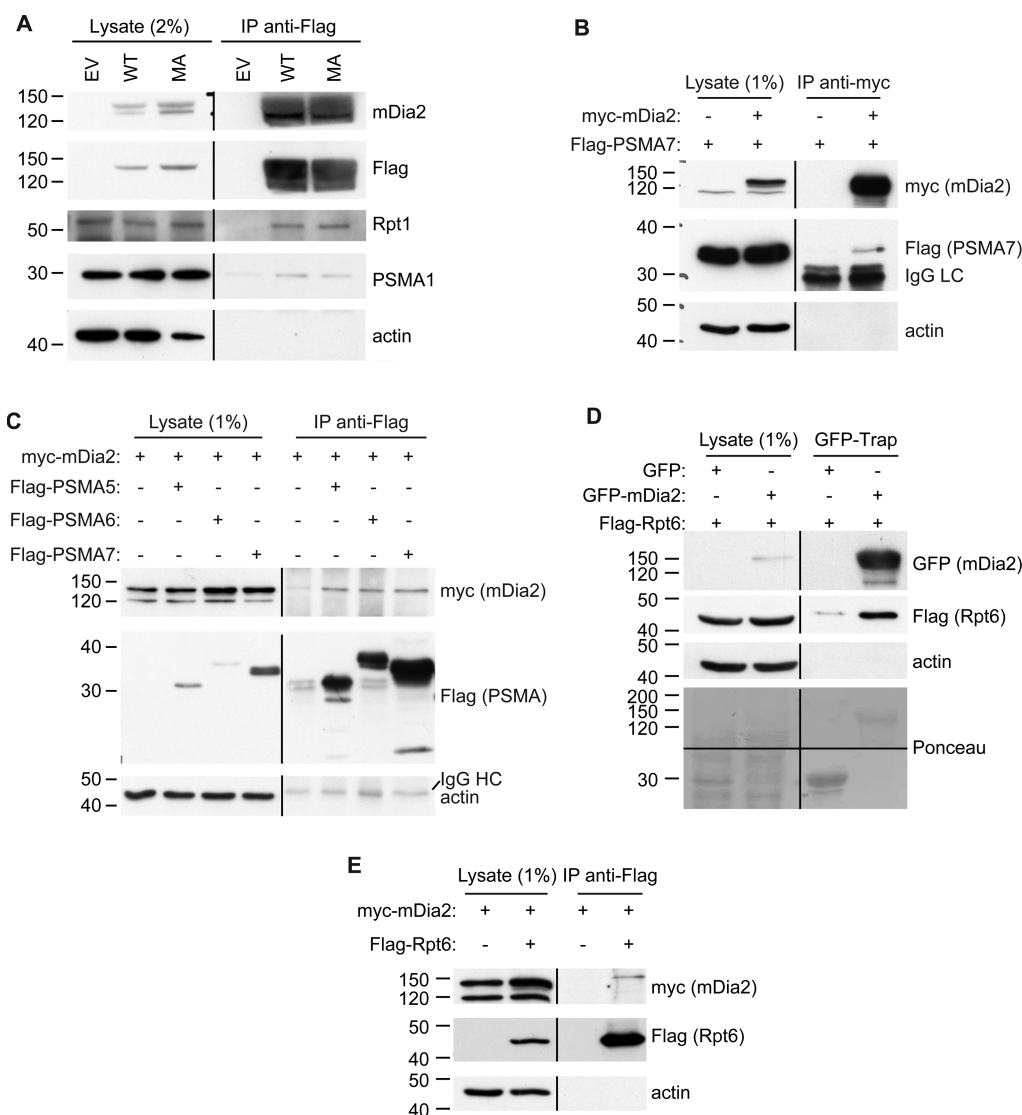


Figure 2. Validation of the proteasome as a genuine mDia2-binding partner. (A) Endogenous proteasome subunits coimmunoprecipitate with mDia2. Experiments were carried out as described in the [Experimental Procedures](#) starting from 1 mg of total cell lysate. Endogenous proteins in the lysates (2%) and the bound material were detected with specific antibodies (on the right). The expression of mDia2 was confirmed using both anti-Flag and anti-mDia2 antibodies. Given that immunoprecipitated mDia2 exceeded the resolution capacity of the gel, the detected bands were slightly smeared above and below the expected molecular weight of Flag-mDia2. One of two experiments that were performed with similar results is shown. (B) PSMA7 coimmunoprecipitates with mDia2. 293T cells were cotransfected with Flag-PSMA7 (+) and either myc-mDia2 (+) or the corresponding empty vector (-). Lysates (1.5 mg) were immunoprecipitated with anti-myc antibodies. Lysates (1%) and affinity-precipitated material were probed as indicated. Cross-reactive IgG light chains (IgG LC) are visible. (C) mDia2 coimmunoprecipitates with PSMA7. 293T cells were cotransfected with myc-mDia2 (+) and either Flag-PSMA7, Flag-PSMA6, or Flag-PSMA5 (+), or the corresponding empty vector (-). Lysates (1.5 mg) were immunoprecipitated with anti-Flag antibodies. Lysates (1%) and affinity-precipitated material were probed as indicated. Note that cross-reactive IgG light chains (IgG LC) of the Flag antibodies migrated slightly faster than those of the Flag-beads used in the other panels. (D) Rpt6 coimmunoprecipitates with mDia2. 293T cells were cotransfected with Flag-Rpt6 (+) and either EGFP-mDia2 (+) or the corresponding empty vector (-). Lysates (1.5 mg) were immunoprecipitated with GFP-trap beads. Lysates (1%) and affinity-precipitated material were probed as indicated. EGFP is visible in the Ponceau, and a horizontal black line marks the removal of the intervening membrane. (E) mDia2 coimmunoprecipitates with Rpt6. 293T cells were cotransfected with myc-mDia2 (+) and either Flag-Rpt6 (+), or the corresponding empty vector (-). Immunoprecipitations were carried out as in panel C using anti-Flag antibodies. One of two (B, D) to three experiments (C, E) that were performed with similar results is shown. All vertical black lines mark the removal of the intervening marker lanes.

the activity of the proteasome in HeLa cells, which thereby showed that the ability to regulate the activity of the proteasome is not a general property of the mDia-family proteins ([Supplemental Figure S4D–F](#)).

Since mDia2 seems to restrain the activity of the proteasome, increased mDia2 levels might be sufficient to inhibit the activity of the proteasome. Given that the other known unconventional function of mDia2 is independent of actin nucleation and

conformation,²² we transfected wild-type mDia2, its MA mutant, the actin-polymerization-deficient I704-to-A (hereafter referred to as IA) and IAMA mutants,^{3,22} or the corresponding empty vector in HeLa cells ([Figure 5A](#)). Although all mDia2 variants were expressed at similar levels and did not affect the expression of the proteasome ([Figure 5A](#)), only mDia2 IAMA significantly reduced the proteolytic activity of the proteasome ([Figure 5B,C](#)). As the actin-depolymerizing drug Latrunculin A did not perturb

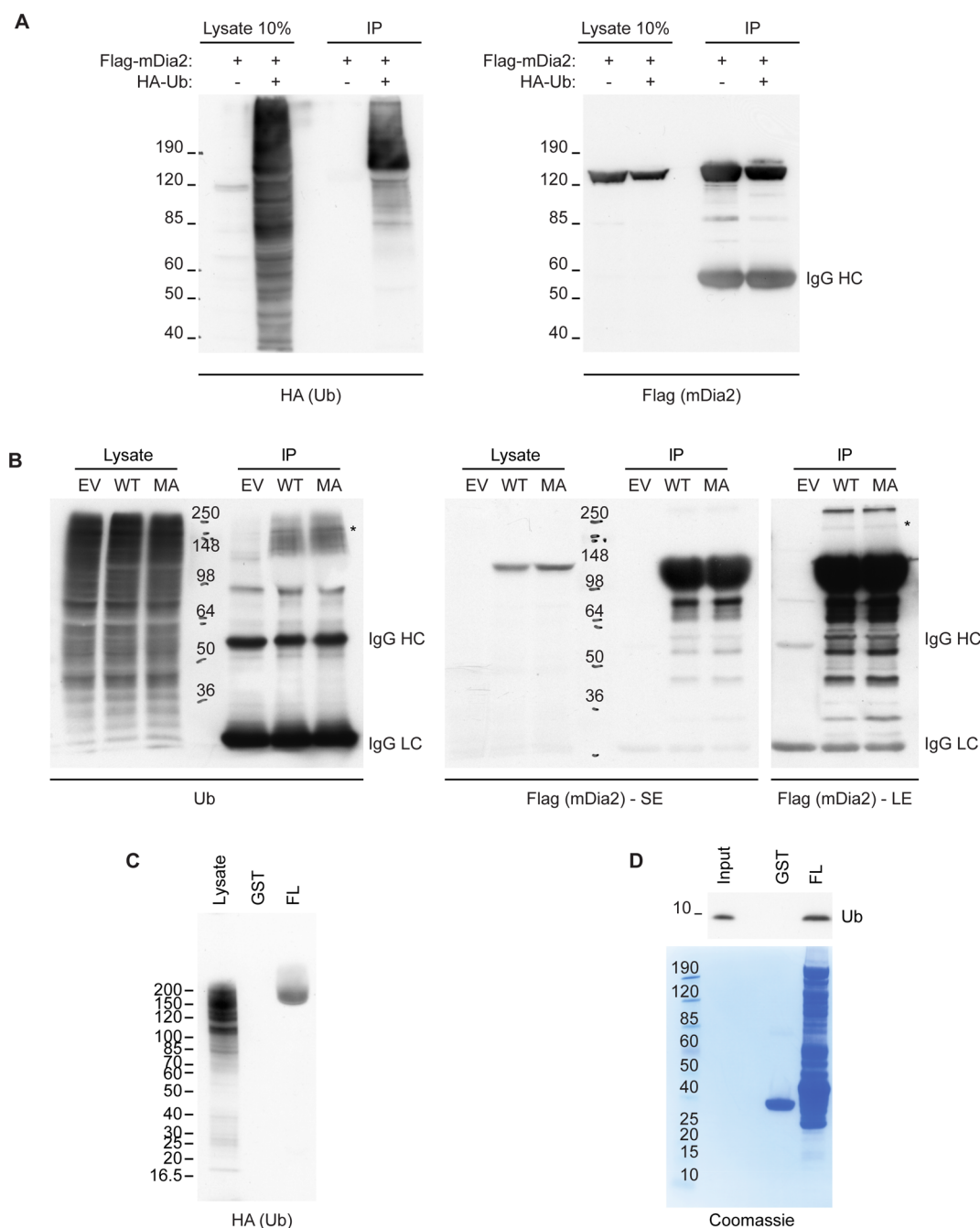


Figure 3. mDia2 is ubiquitinated and binds both conjugated and free Ubiquitin. (A) mDia2 is covalently linked to HA-Ubiquitin. 293T cells were transfected with HA-Ubiquitin (HA-Ub) along with either Flag-tagged wild-type mDia2 (WT) or its MA mutant (MA) or the control empty vector (–). Cells were lysed and, after a freeze–thaw cycle performed to minimize noncovalent protein–protein interactions, lysates (500 μ g) were subjected to immunoprecipitation with anti-Flag antibodies as indicated in the [Experimental Procedures](#) and main text. Lysates (10%) and immunocomplexes were separated by SDS-PAGE and blotted with anti-HA antibodies. After stripping, membranes were probed with anti-Flag antibodies to monitor mDia2 expression. IgG heavy chains (IgG HC) are indicated. One of two experiments that were performed with similar results is shown. (B) mDia2 is polyubiquitinated or monoubiquitinated at multiple sites and associates with endogenous conjugated Ubiquitin. 293T cells were transfected with either Flag-tagged wild-type mDia2 (WT) or its MA mutant (MA) or the empty vector (–). Immunoprecipitation experiments were performed as in panel A using lysates (1.5 mg) in RIPA buffer supplemented with NEM (5 mM), protease, and phosphatase inhibitors. Immunocomplexes were washed extensively with RIPA buffer. Lysates (2%) and immunocomplexes were separated by SDS-PAGE and blotted with anti-Ubiquitin (P4D1) antibodies. After stripping, membranes were probed with anti-Flag antibodies to monitor mDia2 expression. SE and LE: short and long exposure, respectively. Note the ubiquitinated band that also appears in the anti-Flag blot (indicated with an asterisk). IgG heavy chains (IgG HC) and light chains (IgG LC) are indicated. One of three experiments that were performed with similar results is shown. (C) Recombinant full-length mDia2 binds high-molecular weight HA-Ubiquitin conjugates. 293T cells were transfected with HA-Ubiquitin (HA-Ub) and lysed in buffer supplemented with NEM (5 mM), protease, and phosphatase inhibitors. After a freeze–thaw cycle was performed to minimize noncovalent protein–protein interactions, pull-downs were carried out using 500 μ g of lysates and the immobilized full-length GST-mDia2 (FL) or GST (62.5 pmoles). One of two experiments that were performed with similar results is shown. (D) Recombinant mDia2 and free Ubiquitin interact directly in vitro. Purified recombinant free Ubiquitin (4.5 pmoles) was incubated for 2 h at 4 $^{\circ}$ C with immobilized full-length GST-mDia2 (FL) or GST (62.5 pmoles) in 20 μ L. Beads were extensively washed and bound proteins eluted with Laemmli buffer. Input (0.1%) and affinity-precipitated material were separated by SDS-PAGE and blotted with anti-Ubiquitin (P4D1) antibodies. One of two experiments that were performed with similar results is shown.

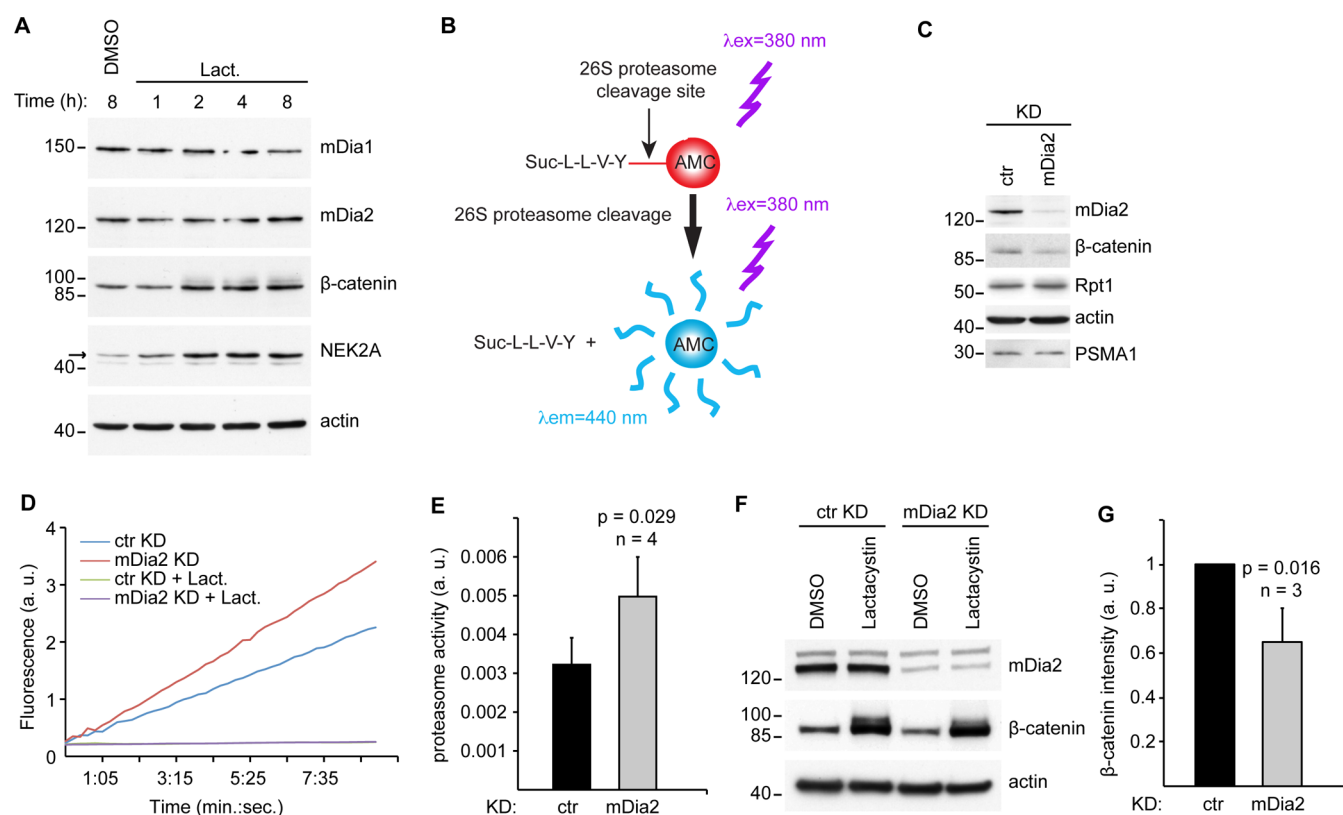


Figure 4. Knockdown of mDia2 increases the activity of the proteasome. (A) mDia2 does not undergo proteasomal degradation. Growing HeLa cells were treated with Lactacystin (Lact., 10 μ M) or DMSO for the indicated time (Time, h = hours). Total cell lysates were prepared, processed, and separated as described in the [Experimental Procedures](#). Expression levels of endogenous mDia2 were detected with specific antibodies. Effectiveness of Lactacystin is demonstrated by the accumulation of endogenous β -catenin and NEK2A (indicated with an arrow), two bona fide proteasome substrates. Actin served as a loading control. One of two experiments that were performed with similar results is shown. (B) Schematic representation of the proteasome activity assay. Suc-L-L-V-Y-AMC (100 μ M) is a fluorogenic peptide and an exogenous substrate used to assay the chymotrypsin-like activity of the proteasome. The proteasome cleaves the amide-bond between the tyrosine (Y) and the fluorogenic reporter group (AMC). Since only free AMC emits light (λ_{em} = 440 nm) upon excitation (λ_{ex} = 380 nm), the increase in fluorescence over time indicates the accumulation of the product (AMC) and can be used as a read-out for the activity of the proteasome. (C) Knockdown of mDia2 does not affect the expression of proteasome subunits. Control (ctr) or mDia2 (mDia2) knockdown (KD) HeLa cells were generated as described in the [Experimental Procedures](#). Total cell lysates (30 μ g) were separated by SDS-PAGE, and the expression of the indicated proteins assessed by immunoblotting. Actin was used as a loading control. (D) Proteasome activity in control (ctr) KD and mDia2 KD cells treated with either DMSO or Lactacystin (10 μ M). AMC fluorescence, expressed as arbitrary units (Fluorescence, a. u.), is plotted against time. The results of a representative experiment are shown. (E) Knockdown of mDia2 results in increased proteasome activity. Proteasome activities (min^{-1}) were determined as described in the [Experimental Procedures](#). Bar graph represents the mean \pm SD (n = 4) and reports the computed p -value. (F) Acute inhibition of the proteasome rescues reduced β -catenin levels in mDia2 knockdown cells. Ctr KD and mDia2 KD cells were treated with either DMSO or Lactacystin (10 μ M) for 5 h. Total cell lysates (30 μ g) were separated by SDS-PAGE and immunoblotted as indicated. Actin was used as a loading control. One of three experiments that were performed with similar results is shown. (G) mDia2 knockdown cells have reduced β -catenin levels. Relative β -catenin levels in panel F were quantified using Quantity One and normalized against the values obtained in the control knockdown cells. Bar graph depicts the mean \pm SD of three independent experiments and the computed p -value.

the activity of the proteasome (not shown), proteasome inhibition by mDia2 IAMA is not an indirect effect of perturbed actin dynamics. This and the observation that the MA mutant was not inhibitory collectively suggest that regulation of the proteasome and actin polymerization by the open conformation of mDia2 are mutually exclusive.

Proteome-Wide Analyses Show That mDia2 Controls the Levels of Ubiquitinated Actin-Regulatory Proteins

To identify potential proteasome substrates regulated by mDia2 in a more unbiased manner, we drew the ubiproteome and the proteome of control and mDia2 knockdown HeLa cells by means of label-free quantitation (LFQ) and liquid chromatography mass spectrometry.⁴⁴

Using anti-FK2 antibodies and a two-step protocol to affinity purify ubiquitinated proteins ([Supplemental Figure 5A](#)), we determined the relative abundance of 785 endogenous proteins

([Supplemental Table S-3](#)). Consistent with the observation that most ubiquitinated proteins are not overtly unstable,⁴⁵ the ubiproteomes were largely independent of mDia2 ([Supplemental Figure 5B](#)). Nevertheless, the abundance of four proteins was consistently altered, and β -catenin was even absent after silencing of mDia2 ([Supplemental Table S-3](#)).

The same cell lysates and label-free approach were used to quantify the total proteome. In this way, we estimated the relative abundance of 4143 proteins in both control and mDia2 knockdown HeLa cells and also found 14 and seven proteins that could be detected exclusively in the former and the latter cells, respectively ([Supplemental Table S-4](#)). Closer inspection of these data indicated that the downregulation of mDia2 affected 3.9% of the identified proteome ([Figure 6A](#) and [Supplemental Table S-4](#)). IPA showed that the proteins downregulated in the mDia2 knockdown cells are involved in well-established

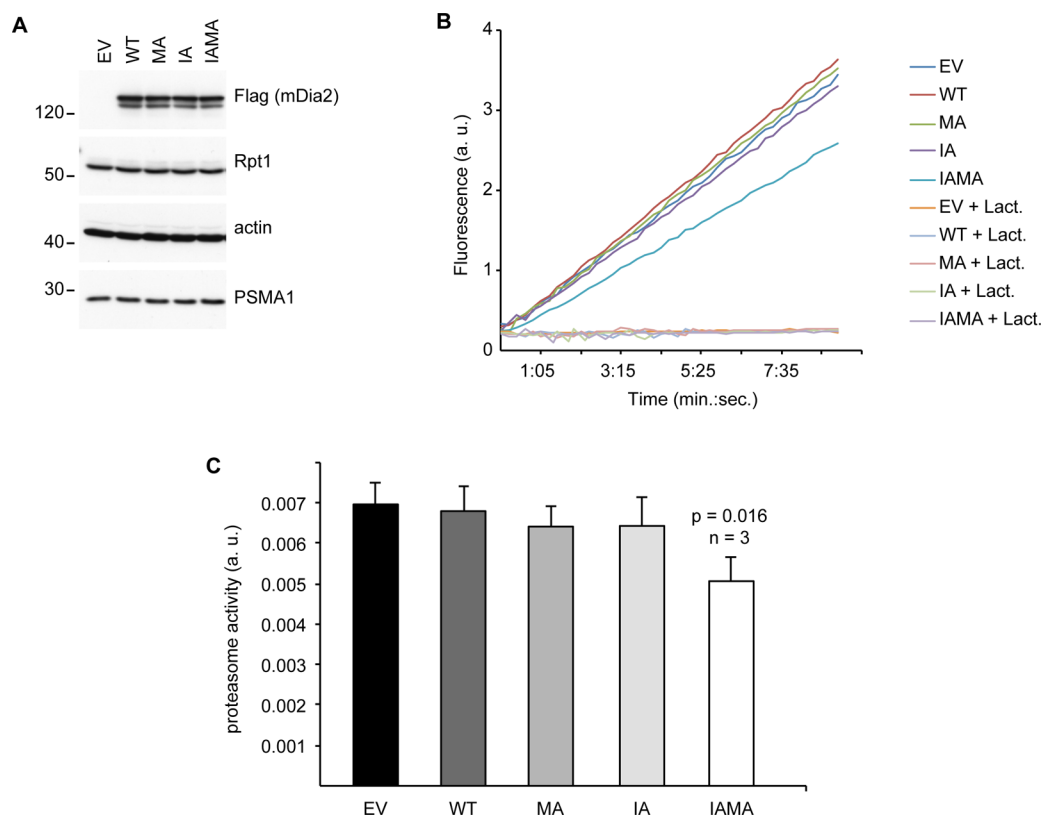


Figure 5. Inhibition of the proteasome is an actin-independent function of the open conformation of mDia2. (A) The overexpression of mDia2 does not alter the expression of endogenous proteasome subunits. HeLa cells were transfected with Flag-tagged mDia2 (WT, MA, IA, and IAMA) or the corresponding empty vector (EV). Transfection efficiencies were monitored by immunofluorescence and were close to 30%. Total cell lysates (30 μ g) were separated by SDS-PAGE. mDia2 and the proteasome protein levels were detected with anti-Flag, anti-Rpt1, and anti-PSMA1 antibodies, respectively. Actin was used as a loading control. One of three experiments that were performed with similar results is shown. (B) Proteasome activity in control and mDia2-overexpressing cells. HeLa cells transfected with empty vector (EV), wild-type mDia2 (WT), active mDia2 (MA), or actin-polymerization-incompetent mDia2 both in the closed and open conformations (IA and IAMA, respectively) and lysates prepared upon treatment with either DMSO or Lactacystin (Lact., 10 μ M). Proteasome assays were performed as indicated in the [Experimental Procedures](#) and results presented as in [Figure 4](#), panel D. The results of a representative experiment are shown. (C) mDia2 IAMA inhibits the proteasome. Proteasome activities were determined as in [Figure 4](#), panel E. Bar graph represents the mean \pm SD ($n = 3$) and includes p -values, if significant.

mDia2-dependent molecular and cellular functions such as cellular movement, cell morphology, cellular assembly and organization, and cell cycle ([Figure 6B](#), [Supplemental Table S-4](#), and [ref 22](#)).

Comparative studies revealed that 18.9% of the proteome was ubiquitinated at the steady state and that the ubiquitome largely overlapped with the proteome (88%) ([Figure 6C](#)). Thus, the remaining part of the ubiquitome (11%) likely consists of low-abundance ubiquitinated proteins that escaped identification ([Figure 6C](#)). The fact that LFQ of the proteome did not reveal a change in β -catenin despite β -catenin being both absent in the anti-FK2 immunocomplexes and downregulated upon RNAi of mDia2 ([Supplemental Table S-3](#) and [Figure 4](#), respectively) suggests that only a small fraction of β -catenin is ubiquitinated in HeLa cells. Interestingly, the proteins that are ubiquitinated and differentially expressed in an mDia2-dependent manner clustered into the cellular assembly and organization, the cellular function and maintenance, the cellular movement, the cellular development, and the cell morphology IPA functional groups ([Figure 6D](#) and [Supplemental Table S-5](#)). Consistently, the associated top canonical pathways were Ephrin receptor signaling and the actin cytoskeleton (data not shown). Therefore, these results strengthen the functional link between the proteasome and mDia2 further suggest that mDia2 can modulate the actin-regulatory ubiquitome.

DISCUSSION

We have used SILAC-based quantitative proteomics as a discovery tool and identified several proteasome subunits, as well as Ubiquitin, as binding partners of both wild-type and active mDia2. Building on this finding, we have employed bioinformatics to describe quantitatively the link between mDia2, Ubiquitin, and the proteasome, two key elements of the UPS. We have experimentally validated these interactions by showing that both Ubiquitin and several proteasome subunits are genuine mDia2-binding proteins. Furthermore, functional analyses relying on proteasome activity assays combined with both loss and gain of function of mDia2 jointly suggest that mDia2, in its open conformation, controls the proteolytic activity of the proteasome only when it does not regulate actin assembly. Finally, we provide evidence that the mDia2-proteasome axis affects the abundance of β -catenin and other ubiquitinated proteins including actin-regulatory proteins.

Importantly, this novel function of mDia2 adds more complexity to the Formin activity cycle. Although the current model postulates that the conversion from the autoinhibited to the open conformation is absolutely required for Drfs to fulfill their functions,² we have demonstrated that autoinhibited mDia2 has a conformation- and actin-independent role in p53 regulation.²² As autoinhibited mDia2 is biologically active, the Formin activity

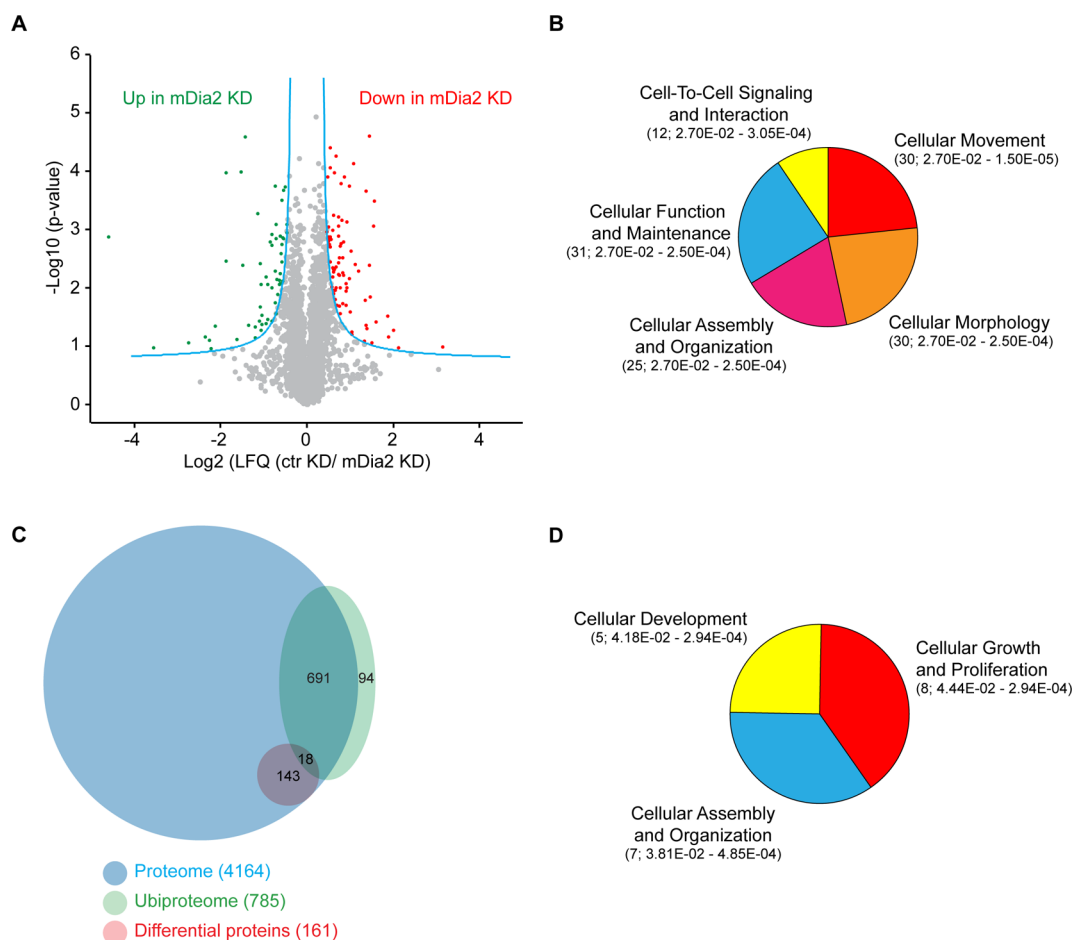


Figure 6. mDia2 regulates the expression of ubiquitinated proteins in HeLa cells. (A) Proteome-wide landscape of control and mDia2 knockdown cells. Control (ctr KD) and mDia2 knockdown (mDia2 KD) HeLa lysates were generated as described in the [Experimental Procedures](#). Upon LC–MS-based label-free quantitation of three biological replicates, significant differentially expressed proteins were identified in Perseus by permutation-based FDR-corrected *t*-test (threshold: $p = 0.05$ and $S_0 = 0.23$). The LFQ intensity of the ctr KD cells over mDia2 KD cells (\log_2 scale) is plotted against the *p*-value (\log_{10} scale). Volcano plot shows the permutation-based FDR threshold as blue lines, each protein listed in [Supplemental Table S-4](#) as a light blue dot, and hallmarks those significantly downregulated and upregulated in the mDia2 knockdown cells in red and green, respectively. (B) Proteins downregulated in the mDia2 knockdown cells cluster into functional groups related to actin dynamics. Downregulated proteins were assigned to pathways regulating biological processes that define a functional group in IPA. Between brackets are number of proteins associated with the indicated functional group; range of Fischer's Exact *t* test *p*-values of the biological processes associated with the indicated functional group ([Supplemental Table S-4](#)). (C) Venn diagram showing the overlap between the proteome and the ubiproteome in HeLa cells and the difference between the control and the mDia2 knockdown cells. Ubiproteomes are depicted in [Supplemental Figure S5](#). (D) The mDia2-regulated ubiproteome clusters into distinct functional groups. Ubiquitinated and differentially expressed proteins from panel C were assigned to pathways regulating biological processes as in panel B.

cycle may include more actin- or conformation-independent functions. In this context, it is remarkable that regulation of the proteasome by mDia2 is possible only when mDia2's open conformation and actin-regulatory abilities are uncoupled. On the basis of these and our previous observations,²² we speculate that the actin-nucleation and the emerging “unconventional” functions of mDia2 may be mutually exclusive.

At the biochemical level, substrate competition cannot be the major mechanism whereby mDia2 inhibits the proteasome because (i) mDia2 is at best a very poor proteasome substrate, and (ii) ubiquitinated proteins largely exceed the total amount of mDia2 present in a cell at any given time ([Supplementary Figure S6](#)). Similarly, the observation that mDia2 attains a low nanomolar concentration in HeLa cells ([Supplementary Figure S6](#)) makes it unlikely that it acts as a noncompetitive inhibitor of the proteasome, which instead accounts for about 0.6% of all total proteins.⁴⁶ Interestingly, the activity of the proteasome in the cell lysates was not affected by the addition of a

large excess of recombinant nonubiquitinated full-length mDia2 produced in bacteria (not shown). This observation supports the above interpretation and suggests that the inhibitory effects resulting from the overexpression of mDia2 IAMA in cells may require ubiquitination of mDia2. To test this hypothesis, we identified and then mutated three ubiquitination sites located in the GBD and the FH2 of mDia2 ([Supplementary Figure S3](#)). However, the high plasticity of the ubiquitination machinery enabled ubiquitination of this mDia2 mutant at alternative sites ([Supplementary Figure S3C](#)) and precluded deeper investigations. Yet, the above considerations are compatible with mDia2 being an exchangeable and substoichiometric proteasome regulator. Consistent with this idea, mDia2 is ubiquitinated and binds Ubiquitin ([Figure 3](#)), bears a Ubiquitin-like domain (the Rho-GTPase-binding domain), and inhibits the activity of the proteasome ([Figure 4](#)) likewise two well-established substoichiometric proteasome regulators, Ubiquitin receptor Rpn10 and Rpn13.^{41,47}

In any case, proteasome inhibition appears to be an exquisite property of mDia2's open conformation. As (i) mDia2 binds to the proteasome in a conformation-independent manner (Figure 1), (ii) the IAMA mutant attains the open conformation, whereas it cannot induce actin polymerization,^{3,48} and (iii) the MA mutant has no noticeable effects on the activity of the proteasome (Figure 5), mDia2 exerts a conformation-specific effect on the proteasome that is incompatible with regulation of actin dynamics. Strikingly, mDia2 seems to control the expression of important actin-regulatory proteins through the proteasome. Thus, the open conformation of mDia2 may influence actin dynamics by both inducing actin polymerization and actin-independent regulation of the proteasome.

On this ground, we propose that the open conformation of mDia2 has at least two functional states, one devoid of and the other endowed with actin-regulatory abilities, which regulate the proteasome and actin assembly, respectively. These observations strongly suggest the existence of yet-unknown nucleation-promoting factors (NPFs) stimulating Drfs' activity on actin and also postulate that NPFs may allow Drfs to change function. Intriguingly, the actin-independent roles of both the closed and open conformations of mDia2 may contribute to the tumor-suppressor and antimetastatic activities ascribed to this Drf protein.^{12,49}

Finally, proteasome regulation by mDia2 may be relevant for predicting response to therapy in prostate cancer patients. Given that deletion of DIAPH3 (the human homologue of mouse mDia2) is common in aggressive prostate cancers with poor outcome^{12,49} and proteasome inhibitor Bortezomib is used to treat both local and advanced androgen-independent prostate cancer,^{50,51} mDia2 expression levels may predict response to Bortezomib and guide personalized treatment of prostate cancer patients. Although this hypothesis awaits formal experimental verification, the unconventional role of mDia2 in proteasome regulation identified herein sheds new light on the pathophysiological functions of mDia2.

■ ASSOCIATED CONTENT

Supporting Information

The Supporting Information is available free of charge on the ACS Publications website at DOI: 10.1021/acs.jproteome.6b00718.

Supplemental figures (PDF)

mDia2-binding proteins ranked according to log₂ H/L ratio computed using forward and reverse experiments (XLSX)

GO analysis of mDia2-interactomes (XLSX)

Inventory of ubiquiproteome isolated from control and mDia2 knockdown HeLa cells (XLSX)

Inventory of proteome isolated from control and mDia2 knockdown HeLa cells (XLSX)

Inventory of ubiquitinated proteins whose expression changes upon mDia2 knockdown and IPA analysis thereof (XLSX)

■ AUTHOR INFORMATION

Corresponding Authors

*E-mail: m.altelaar@uu.nl. Phone: +31 30 2539554.

*E-mail: m.innocenti@nki.nl. Phone: +31 20 5121976.

Author Contributions

^{||}T.I. and R.v.d.K. contributed equally to this work. R.v.d.K. performed the AP-MS screen. A.F.M.A., O.B.B., S.S.G., and

A.F.M.A. carried out the MS and network analyses. T.I., R.v.d.K., E.A., and M.I. were involved in both the validations and the functional assays. M.I. conceived and supervised the project and wrote the manuscript.

Notes

The authors declare no competing financial interest.

The mass spectrometry data have been deposited to the ProteomeXchange Consortium³⁵ through the PRIDE partner repository (Project accession, PXD002066; Username, reviewer54687@ebi.ac.uk; Password, mrtfepq3).

■ ACKNOWLEDGMENTS

We thank J. Neefjes, R. Wolthuis, A. Bertolotti, N. A. Barlev, and T. Sixma who generously provided us with reagents. We also thank Linsey R. Raaijmakers and Martin A. Fitzpatrick for help with Cytoscape. M.I. was supported by a grant from the Cancer Genomics Centre (CGC 2009-2013). A.F.M.A. was supported by The Netherlands Organization for Scientific Research (NWO) with a VIDI grant (723.012.102). This work is part of the project Proteins At Work, financed by NWO as part of the National Roadmap Large-scale Research Facilities of The Netherlands (Project No. 184.032.201).

■ REFERENCES

- (1) Schonichen, A.; Geyer, M. Fifteen formins for an actin filament: a molecular view on the regulation of human formins. *Biochim. Biophys. Acta, Mol. Cell Res.* **2010**, *1803* (2), 152–63.
- (2) Chesarone, M. A.; DuPage, A. G.; Goode, B. L. Unleashing formins to remodel the actin and microtubule cytoskeletons. *Nat. Rev. Mol. Cell Biol.* **2010**, *11* (1), 62–74.
- (3) Bartolini, F.; Moseley, J. B.; Schmoranz, J.; Cassimeris, L.; Goode, B. L.; Gundersen, G. G. The formin mDia2 stabilizes microtubules independently of its actin nucleation activity. *J. Cell Biol.* **2008**, *181* (3), 523–36.
- (4) Aspenstrom, P. Formin-binding proteins: modulators of formin-dependent actin polymerization. *Biochim. Biophys. Acta, Mol. Cell Res.* **2010**, *1803* (2), 174–82.
- (5) Peng, J.; Wallar, B. J.; Flanders, A.; Swiatek, P. J.; Alberts, A. S. Disruption of the Diaphanous-related formin Drf1 gene encoding mDia1 reveals a role for Drf3 as an effector for Cdc42. *Curr. Biol.* **2003**, *13* (7), 534–45.
- (6) Nezami, A.; Poy, F.; Toms, A.; Zheng, W.; Eck, M. J. Crystal structure of a complex between amino and carboxy terminal fragments of mDia1: insights into autoinhibition of diaphanous-related formins. *PLoS One* **2010**, *5* (9), e12992.
- (7) Otomo, T.; Tomchick, D. R.; Otomo, C.; Machius, M.; Rosen, M. K. Crystal structure of the Formin mDia1 in autoinhibited conformation. *PLoS One* **2010**, *5* (9), e12896.
- (8) Wallar, B. J.; Stropich, B. N.; Schoenherr, J. A.; Holman, H. A.; Kitchen, S. M.; Alberts, A. S. The basic region of the diaphanous-autoregulatory domain (DAD) is required for autoregulatory interactions with the diaphanous-related formin inhibitory domain. *J. Biol. Chem.* **2006**, *281* (7), 4300–7.
- (9) Beli, P.; Mascheroni, D.; Xu, D.; Innocenti, M. WAVE and Arp2/3 jointly inhibit filopodium formation by entering into a complex with mDia2. *Nat. Cell Biol.* **2008**, *10* (7), 849–57.
- (10) Yang, C.; Czech, L.; Gerboth, S.; Kojima, S.; Scita, G.; Svitkina, T. Novel roles of formin mDia2 in lamellipodia and filopodia formation in motile cells. *PLoS Biol.* **2007**, *5* (11), e317.
- (11) Eisenmann, K. M.; Harris, E. S.; Kitchen, S. M.; Holman, H. A.; Higgs, H. N.; Alberts, A. S. Dia-interacting protein modulates formin-mediated actin assembly at the cell cortex. *Curr. Biol.* **2007**, *17* (7), 579–91.
- (12) Di Vizio, D.; Kim, J.; Hager, M. H.; Morello, M.; Yang, W.; Lafargue, C. J.; True, L. D.; Rubin, M. A.; Adam, R. M.; Beroukhim, R.; Demicheli, F.; Freeman, M. R. Oncosome formation in prostate cancer:

association with a region of frequent chromosomal deletion in metastatic disease. *Cancer Res.* **2009**, *69* (13), 5601–9.

(13) Innocenti, M.; Isogai, T.; Jalink, K.; Kedziora, K. M. Invadosomes - shaping actin networks to follow mechanical cues. *Front. Biosci., Landmark Ed.* **2016**, *21*, 1092–117.

(14) Narumiya, S.; Tanji, M.; Ishizaki, T. Rho signaling, ROCK and mDia1, in transformation, metastasis and invasion. *Cancer Metastasis Rev.* **2009**, *28* (1–2), 65–76.

(15) Nurnberg, A.; Kitzing, T.; Grosse, R. Nucleating actin for invasion. *Nat. Rev. Cancer* **2011**, *11* (3), 177–87.

(16) Ji, P.; Jayapal, S. R.; Lodish, H. F. Enucleation of cultured mouse fetal erythroblasts requires Rac GTPases and mDia2. *Nat. Cell Biol.* **2008**, *10* (3), 314–21.

(17) Wallar, B. J.; Deward, A. D.; Resau, J. H.; Alberts, A. S. RhoB and the mammalian Diaphanous-related formin mDia2 in endosome trafficking. *Exp. Cell Res.* **2007**, *313* (3), 560–71.

(18) Watanabe, S.; Ando, Y.; Yasuda, S.; Hosoya, H.; Watanabe, N.; Ishizaki, T.; Narumiya, S. mDia2 induces the actin scaffold for the contractile ring and stabilizes its position during cytokinesis in NIH 3T3 cells. *Mol. Biol. Cell* **2008**, *19* (5), 2328–38.

(19) Baarlink, C.; Wang, H.; Grosse, R. Nuclear actin network assembly by formins regulates the SRF coactivator MAL. *Science* **2013**, *340* (6134), 864–7.

(20) Bartolini, F.; Gundersen, G. G. Formins and microtubules. *Biochim. Biophys. Acta, Mol. Cell Res.* **2010**, *1803* (2), 164–73.

(21) Destaing, O.; Saltel, F.; Gilquin, B.; Chabadel, A.; Khochbin, S.; Ory, S.; Jurdic, P. A novel Rho-mDia2-HDAC6 pathway controls podosome patterning through microtubule acetylation in osteoclasts. *J. Cell Sci.* **2005**, *118* (13), 2901–11.

(22) Isogai, T.; van der Kammen, R.; Goerdal, S. S.; Heck, A. J.; Altelaar, A. F.; Innocenti, M. Proteomic analyses uncover a new function and mode of action for mouse homolog of Diaphanous 2 (mDia2). *Mol. Cell. Proteomics* **2015**, *14* (4), 1064–78.

(23) Shibue, T.; Brooks, M. W.; Inan, M. F.; Reinhardt, F.; Weinberg, R. A. The outgrowth of micrometastases is enabled by the formation of filopodium-like protrusions. *Cancer Discovery* **2012**, *2* (8), 706–21.

(24) Schoen, C. J.; Emery, S. B.; Thorne, M. C.; Ammana, H. R.; Sliwerska, E.; Arnett, J.; Hortsch, M.; Hannan, F.; Burmeister, M.; Lesperance, M. M. Increased activity of Diaphanous homolog 3 (DIAPH3)/diaphanous causes hearing defects in humans with auditory neuropathy and in *Drosophila*. *Proc. Natl. Acad. Sci. U. S. A.* **2010**, *107* (30), 13396–401.

(25) Ong, S. E.; Mann, M. A practical recipe for stable isotope labeling by amino acids in cell culture (SILAC). *Nat. Protoc.* **2007**, *1* (6), 2650–60.

(26) Altelaar, A. F.; Munoz, J.; Heck, A. J. Next-generation proteomics: towards an integrative view of proteome dynamics. *Nat. Rev. Genet.* **2012**, *14* (1), 35–48.

(27) Isogai, T.; van der Kammen, R.; Innocenti, M. SMIFH2 has effects on Formins and p53 that perturb the cell cytoskeleton. *Sci. Rep.* **2015**, *5*, 9802.

(28) Isogai, T.; van der Kammen, R.; Leyton-Puig, D.; Kedziora, K. M.; Jalink, K.; Innocenti, M. Initiation of lamellipodia and ruffles involves cooperation between mDia1 and the Arp2/3 complex. *J. Cell Sci.* **2015**, *128* (20), 3796–810.

(29) Galovic, M.; Xu, D.; Areces, L. B.; van der Kammen, R.; Innocenti, M. Interplay between N-WASP and CK2 optimizes clathrin-mediated endocytosis of EGFR. *J. Cell Sci.* **2011**, *124* (12), 2001–12.

(30) Wisniewski, J. R.; Zougman, A.; Nagaraj, N.; Mann, M. Universal sample preparation method for proteome analysis. *Nat. Methods* **2009**, *6* (5), 359–62.

(31) Frese, C. K.; Altelaar, A. F.; Hennrich, M. L.; Nolting, D.; Zeller, M.; Griep-Raming, J.; Heck, A. J.; Mohammed, S. Improved peptide identification by targeted fragmentation using CID, HCD and ETD on an LTQ-Orbitrap Velos. *J. Proteome Res.* **2011**, *10* (5), 2377–88.

(32) Bleijerveld, O. B.; Wijten, P.; Cappadona, S.; McClellan, E. A.; Polat, A. N.; Raijmakers, R.; Sels, J. W.; Colle, L.; Grasso, S.; van den Toorn, H. W.; van Breukelen, B.; Stubbs, A.; Pasterkamp, G.; Heck, A. J.; Hoefer, I. E.; Scholten, A. Deep proteome profiling of circulating

granulocytes reveals bactericidal/permeability-increasing protein as a biomarker for severe atherosclerotic coronary stenosis. *J. Proteome Res.* **2012**, *11* (11), 5235–44.

(33) Cox, J.; Mann, M. MaxQuant enables high peptide identification rates, individualized p.p.b.-range mass accuracies and proteome-wide protein quantification. *Nat. Biotechnol.* **2008**, *26* (12), 1367–72.

(34) Deeb, S. J.; D'Souza, R. C.; Cox, J.; Schmidt-Supprian, M.; Mann, M. Super-SILAC allows classification of diffuse large B-cell lymphoma subtypes by their protein expression profiles. *Mol. Cell. Proteomics* **2012**, *11* (5), 77–89.

(35) Vizcaino, J. A.; Deutsch, E. W.; Wang, R.; Csordas, A.; Reisinger, F.; Rios, D.; Dienes, J. A.; Sun, Z.; Farrar, T.; Bandeira, N.; Binz, P. A.; Xenarios, I.; Eisenacher, M.; Mayer, G.; Gatto, L.; Campos, A.; Chalkley, R. J.; Kraus, H. J.; Albar, J. P.; Martinez-Bartolome, S.; Apweiler, R.; Omenn, G. S.; Martens, L.; Jones, A. R.; Hermjakob, H. ProteomeXchange provides globally coordinated proteomics data submission and dissemination. *Nat. Biotechnol.* **2014**, *32* (3), 223–6.

(36) Huang, da, W.; Sherman, B. T.; Lempicki, R. A. Systematic and integrative analysis of large gene lists using DAVID bioinformatics resources. *Nat. Protoc.* **2008**, *4* (1), 44–57.

(37) Szklarczyk, D.; Franceschini, A.; Kuhn, M.; Simonovic, M.; Roth, A.; Minguez, P.; Doerks, T.; Stark, M.; Muller, J.; Bork, P.; Jensen, L. J.; von Mering, C. The STRING database in 2011: functional interaction networks of proteins, globally integrated and scored. *Nucleic Acids Res.* **2011**, *39* (Database), D561–8.

(38) Cline, M. S.; Smoot, M.; Cerami, E.; Kuchinsky, A.; Landys, N.; Workman, C.; Christmas, R.; Avila-Campilo, I.; Creech, M.; Gross, B.; Hanspers, K.; Isserlin, R.; Kelley, R.; Killcoyne, S.; Lotia, S.; Maere, S.; Morris, J.; Ono, K.; Pavlovic, V.; Pico, A. R.; Vailaya, A.; Wang, P. L.; Adler, A.; Conklin, B. R.; Hood, L.; Kuiper, M.; Sander, C.; Schumlevich, I.; Schwikowski, B.; Warner, G. J.; Ideker, T.; Bader, G. D. Integration of biological networks and gene expression data using Cytoscape. *Nat. Protoc.* **2007**, *2* (10), 2366–82.

(39) Kisselev, A. F.; Goldberg, A. L. Monitoring activity and inhibition of 26S proteasomes with fluorogenic peptide substrates. *Methods Enzymol.* **2005**, *398*, 364–78.

(40) Bustos, D.; Bakalarski, C. E.; Yang, Y.; Peng, J.; Kirkpatrick, D. S. Characterizing ubiquitination sites by peptide-based immunoaffinity enrichment. *Mol. Cell. Proteomics* **2012**, *11* (12), 1529–40.

(41) Schmidt, M.; Finley, D. Regulation of proteasome activity in health and disease. *Biochim. Biophys. Acta, Mol. Cell Res.* **2014**, *1843* (1), 13–25.

(42) Hames, R. S.; Wattam, S. L.; Yamano, H.; Bacchieri, R.; Fry, A. M. APC/C-mediated destruction of the centrosomal kinase Nek2A occurs in early mitosis and depends upon a cyclin A-type D-box. *EMBO J.* **2001**, *20* (24), 7117–27.

(43) DeWard, A. D.; Alberts, A. S. Ubiquitin-mediated degradation of the formin mDia2 upon completion of cell division. *J. Biol. Chem.* **2009**, *284* (30), 20061–9.

(44) Boersema, P. J.; Raijmakers, R.; Lemeer, S.; Mohammed, S.; Heck, A. J. Multiplex peptide stable isotope dimethyl labeling for quantitative proteomics. *Nat. Protoc.* **2009**, *4* (4), 484–94.

(45) Kim, W.; Bennett, E. J.; Huttlin, E. L.; Guo, A.; Li, J.; Possemato, A.; Sowa, M. E.; Rad, R.; Rush, J.; Comb, M. J.; Harper, J. W.; Gygi, S. P. Systematic and quantitative assessment of the ubiquitin-modified proteome. *Mol. Cell* **2011**, *44* (2), 325–40.

(46) Wojcik, C.; DeMartino, G. N. Intracellular localization of proteasomes. *Int. J. Biochem. Cell Biol.* **2003**, *35* (5), 579–89.

(47) Hamazaki, J.; Hirayama, S.; Murata, S. Redundant Roles of Rpn10 and Rpn13 in Recognition of Ubiquitinated Proteins and Cellular Homeostasis. *PLoS Genet.* **2015**, *11* (7), e1005401.

(48) Alberts, A. S. Identification of a carboxyl-terminal diaphanous-related formin homology protein autoregulatory domain. *J. Biol. Chem.* **2001**, *276* (4), 2824–30.

(49) Hager, M. H.; Morley, S.; Bielenberg, D. R.; Gao, S.; Morello, M.; Holcomb, I. N.; Liu, W.; Mouneimne, G.; Demicheli, F.; Kim, J.; Solomon, K. R.; Adam, R. M.; Isaacs, W. B.; Higgs, H. N.; Vessella, R. L.; Di Vizio, D.; Freeman, M. R. DIAPH3 governs the cellular transition to the amoeboid tumour phenotype. *EMBO Mol. Med.* **2012**, *4*, 743.

(50) Papandreou, C. N.; Logothetis, C. J. Bortezomib as a potential treatment for prostate cancer. *Cancer Res.* **2004**, *64* (15), 5036–43.

(51) Voutsadakis, I. A.; Papandreou, C. N. The ubiquitin-proteasome system in prostate cancer and its transition to castration resistance. *Urol Oncol* **2012**, *30* (6), 752–61.